from its cloud top value of 100 m/sec (the so-called 4-day rotation), which reflects a balanced cyclostrophic flow, to nearly zero by about 80 km. This decrease (Fig. 3) is balanced by an increase in the advection and viscosity terms in the meridional momentum equation, and it reflects the diminishing role of cyclostrophic forces. This causes the mean meridional component of the wind to become large (60 m/sec) above 80 km, as shown in Fig. 3a.

Infrared imaging of the planet (Fig. 4) has revealed a great deal of fascinating structure, especially at the cloud top and in the polar region. Dark bands of high, cold cloud containing spiral filaments form a "collar" around the pole centered on approximately 65°N. The thickness of this feature varies with longitude and its detailed structure with time; its widest part is some 2000 km across, and this maximum appears to be phase-locked to the sun. The polar collar clouds in general are optically thick in the infrared and extend up to altitudes of 75 km. Inversion of multiple zenith measurements shows that this increase in effective cloud height is due either to an increase in the scale height of the cloud, from around 2 km, which is typical of most of the planet, to around 6 or 7 km in the polar collar, or to a second discrete layer overlying the main deck. The cloud opacity shows a marked wavelength dependence in the region 11 to 15 μm: everywhere outside the collar region the 11.5-μm brightness temperature is higher than that observed at 13 μm, but in the collar cloud this situation reverses. Numerical simulations in which multiple scattering algorithms are used to solve for the radiated intensity as a function of wavelength and angle show that the refractive index of an aqueous solution of 75 percent H_2SO_4 is sufficiently different at 11.5 and 13 μm to account for this observation. In particular, a model cloud with droplets 1 to 2 μm in radius is capable of fitting the data for certain distributions of number density with altitude.

Within the collar clouds, two bright features are located to either side of the pole. Fourier analysis of maps from successive orbits shows that the motion of this "dipole" can be interpreted, on average, as a retrograde motion about the pole with a 2.7-day period. This period matches well the observed average period of rotation of small-scale ultraviolet features seen at high latitudes in Mariner 10 images (*8*). However, both the rotation period of the dipole and the position of its axis relative to the pole appear to be variable from day to day. The 11.5-μm temperatures within the bright "eyes" approach 260 K, the highest observed anywhere on the planet in this wavelength region, suggesting that they correspond to a lowering or clearing of the main cloud deck (*9*). Temperatures are higher in the atmosphere overlying the hot regions up to altitudes of at least 80 km, probably due to heating by thermal radiation from below. The two eyes are joined, in some of the images, by a bright S-shaped filament that passes near the center of rotation. Other bright filaments are sometimes seen extending across the cold collar cloud from one or the other eye. No ready explanation offers itself for these phenomena, but it is apparent that a simple vortex structure is no longer sufficient to explain the cloud structure at the pole. At the very least, such a circulation must be modified by a wavenumber 2 phenomenon surrounding the pole. We note in passing that wavenumber 2 disturbances are present in the terrestrial stratosphere in the form of Kelvin waves and tides (*10*), and that they play an important role in such phenomena as sudden warmings and the quasi-biennial oscillation. Furthermore, there is preliminary evidence for wavenumber 2 structure in equatorial and midlatitude regions on Venus from our temperature maps.

Finally, a preliminary analysis of data from the observations of reflected sunlight in the 0.4- to 5.0-μm albedo and 2.0-μm cloud height channels is strongly suggestive of the presence of a thin haze high above the main cloud deck. This haze covers the entire planet, including the polar collar and dipole features. The particle size is less than 0.5 μm, assuming spherical particles with refractive indices appropriate to a 75 percent H_2SO_4 solution. This haze presumably is the same as that reported by Martonchik and Beer (*11*) from ground-based near-infrared spectroscopy.

F. W. TAYLOR
D. J. DINER, L. S. ELSON
D. J. MCCLEESE, J. V. MARTONCHIK
Earth and Space Sciences Division, Jet Propulsion Laboratory, California Institute of Technology, Pasadena 91103
J. DELDERFIELD
S. P. BRADLEY, J. T. SCHOFIELD
Atmospheric Physics Department, University of Oxford, Oxford, England
J. C. GILLE, M. T. COFFEY
National Center for Atmospheric Research, Boulder, Colorado 80302

References and Notes

1. F. W. Taylor *et al.*, *Science* **203**, 779 (1979).
2. F. W. Taylor, *Appl. Opt.* **13**, 1559 (1974).
3. J. C. Gille and F. B. House, *J. Atmos. Sci.* **28**, 1427 (1971); J. C. Gille, P. L. Bailey, J. M. Russell, in preparation.
4. O. J. Yakovlev, A. I. Efimov, S. S. Matyugov, T. S. Timofeeva, E. V. Chub, G. D. Yakovleva, *Cosm. Res. (USSR)* **16**, 113 (1978).
5. G. M. Keating, F. W. Taylor, J. Y. Nicholson, E. W. Hinson, *Science* **205**, 62 (1979).
6. F. W. Taylor, *J. Atmos. Sci.* **32**, 1101 (1975).
7. L. S. Elson, *Geophys. Astrophys. Fluid. Dyn.* **10**, 319 (1978); in preparation.
8. S. Limaye and V. E. Suomi, *Bull. Am. Astron. Soc.* **9**, 509 (1977).
9. F. W. Taylor, D. J. McCleese, D. J. Diner, *Nature (London)*, in press.
10. J. R. Holton, *An Introduction to Dynamical Meterology* (Academic Press, New York, 1972).
11. J. V. Martonchik and R. Beer, *J. Atmos. Sci.* **32**, 1151 (1975).
12. In addition to those acknowledged in our earlier report (*1*), we would like to thank the personnel in the JPL Photography Laboratory, especially D. Deats and R. Post, who have taken special pains on our behalf; the personnel of the NASA Communications Network at Jet Propulsion Laboratory, Goddard Spaceflight Center, Madrid, and London for supporting daily JPL-Oxford computer linkups; and R. Fimmel, J. Ferandin, and F. Schutz for their support. D.J.D. is a NASA-NRC Resident Research Associate. This report represents one phase of work carried out at the Jet Propulsion Laboratory, California Institute of Technology, under NASA contract NAS 7-100. The Oxford University contribution was funded by the U.K. Science Research Council.

15 May 1979

Further Results of the Pioneer Venus Nephelometer Experiment

Abstract. *Backscattering data for the nephelometer experiments conducted aboard the Pioneer Venus mission probes, including data up to the highest altitudes measured by the probes, are presented. A few small signals were detected below the main cloud deck. Ambient radiation was measured at near-ultraviolet and visible wavelengths; the variation of extinction of near-ultraviolet with altitude is inferred. Ambient radiance decreased more rapidly at 530 than at 745 nanometers in the lower atmosphere.*

In this report we present a more complete set of backscattering data than was available earlier (*1, 2*). In addition, we present data from the ultraviolet (UV) and visible channel radiometer experiments that were incorporated into the nephelometer instrument.

The results of the backscattering nephelometer measurements in the cloud regions are shown in Fig. 1. For comparison purposes, the data from each of the probes are plotted as a function of altitude above the sounder probe landing site (*3*). Although the protective window

0036-8075/79/0706-0067$00.50/0

covers of each of the probe nephelometers were deployed at approximately the same time after the deceleration pulse, the different entrance trajectories gave rise to deployment altitudes of about 66, 64, and 61 km for the day, night, and north probes, respectively. The sounder probe nephelometer was deployed automatically when the heat shield was jettisoned, at an altitude of about 65 km.

In accord with our results and the results of Marov *et al.* (*4*) the cloud data show gross features that appear to be planetary in nature, although details appear to vary from one location to another. The cloud at the sounder probe location was clearly stratified into four distinct regions (*1*, *5*, *6*); the essential structure of this stratification appears to carry over to the other probe locations.

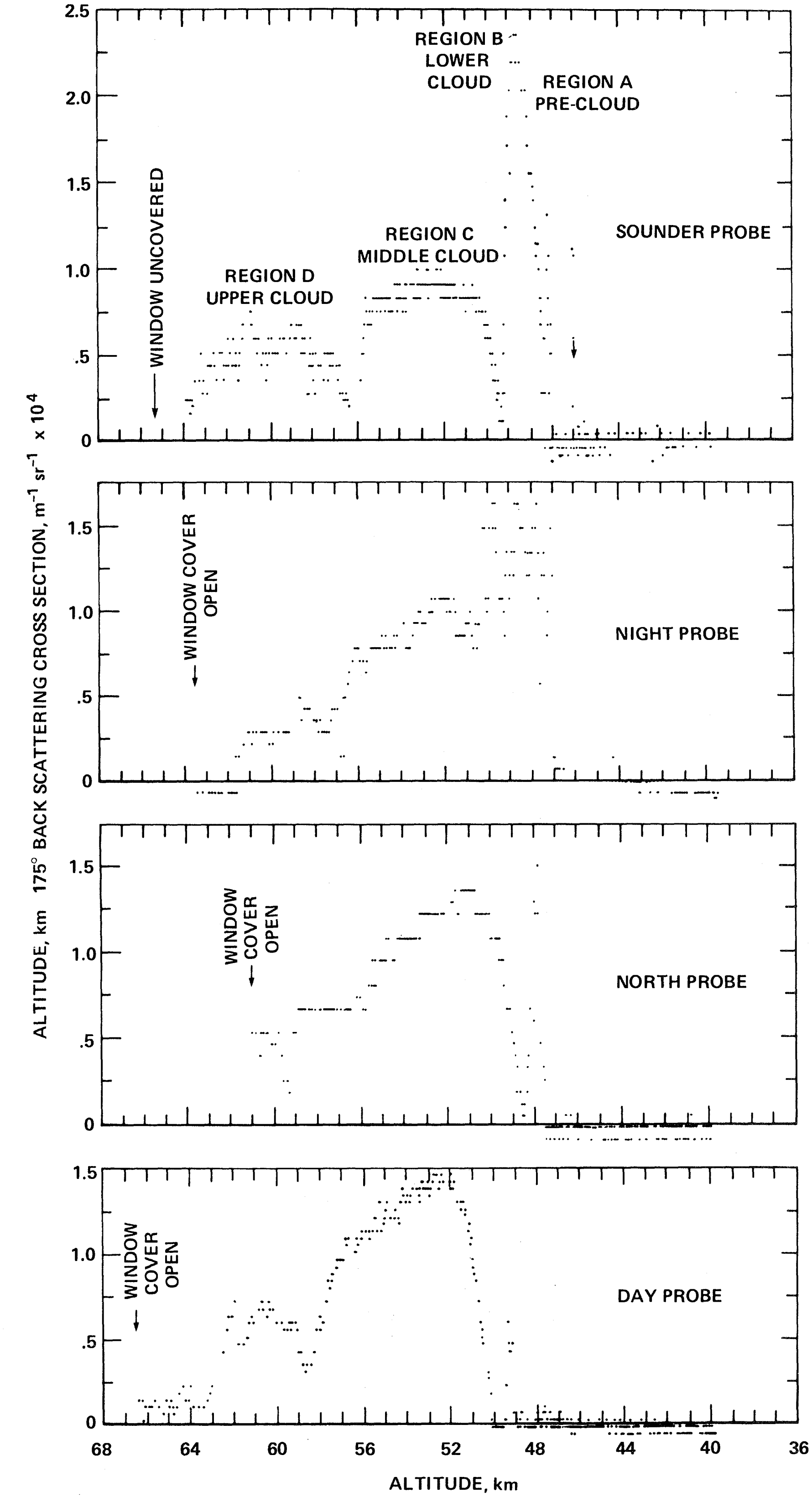

Fig. 1. Plots of the 175° backscattering cross sections versus altitude for the sounder, night, north, and day probe nephelometers. Altitudes have been referenced to the elevation of the impact location of the sounder probe.

The backscattering measurements permit five observations:

1) At the highest altitudes (earlier labeled region D or upper cloud) the data obtained for the sounder and day probes indicate an inhomogeneous or patchy consistency (as is also hinted from the results of the radiation experiments discussed below), with a sharp increase in the backscatter signal evident at 63 km for the day probe and at 64 km for the sounder probe. The night probe descended from its deployment altitude of 63.6 to 61.7 km in a relatively particulate-free atmosphere before it encountered any appreciable backscattering material. Our data for the corresponding region in the sounder probe are consistent with a value of 1.44 for the index of refraction for nonabsorbing spherical particles at a wavelength of 900 nm. This number is derived by computing the 175° backscattering cross section for the particle-size distribution given by Knollenberg and Hunten (*5*, *6*) for this region, with the same index of refraction used as a parameter for all of the particles and comparison of these calculations with our data shown in Fig. 1.

2) The next lower region (earlier labeled region C or middle cloud) appears to be a planetary feature. It is separated at 56 to 58 km from region D by a "trough" and is characterized throughout its extent—except at the sounder probe location, where the backscattering intensity is constant with altitude—by an increase with diminishing altitude. On the sounder probe, a comparison of our data with the tabulated size distribution of particles obtained by the cloud particle size spectrometer (*5*, *6*) shows an excellent fit when an index of refraction of 1.40 is used for the large particles [mode 3 of (*6*)] and one of 1.44 for the smaller particles [modes 1 and 2 of (*6*)] and under an assumption of nonabsorbing spherical particles. The marginal effect of small particles on scattering properties makes possible a larger domain of values for their index; the same is true for region B. For these calculations, however, we have assumed that the smaller particles in cloud regions B, C, and D are similar in composition. This assumption has little effect on the index derived for the larger particles in region C.

3) Below, the region earlier labeled region B or lower cloud (about 51 to 48 km), appears to be the most variable. It is the densest at the sounder and night probe locations (50 percent larger for the sounder probe) but is nearly absent at the day and north probe locations. Comparison with data obtained from our radiometer channels seems to indicate that the material present in this region at the sounder probe locations may be found lower in the atmosphere, at least for the day probe. From the particulate size distribution obtained on the sounder probe (*5*, *6*) and by comparison with our data, we compute a value of 1.32 for the index of refraction of the large particles [mode 3 of (*6*)] present in this location, using 1.44 for the small and medium-sized particles [modes 1 and 2 of (*6*)] (or slightly above 1.33 if all the particles are assumed to have the same index), if all the particles are spherical and nonabsorbing. If the large particles are solid and their symmetry far from spherical, this index may be larger.

4) The lowest region (earlier labeled region A or precloud) is composed of small particles [mode 1 of (*6*)] inferred to be concentrated H_2SO_4 at the sounder probe location (*1*). Thin strata appearing below the main cloud bank at other probe locations are presumed to be similar in composition to those found at the sounder probe location. The base of cloud region B occurs at all of the locations at altitudes of about 47 to 49 km.

5) The region below about 45 km—that is, below the main cloud deck—is relatively free of 175° backscattering material with the exceptions noted below. The night probe nephelometer detected a very thin stratum at about 44.3 km and a very small amount of material at an altitude between 6.0 and 5.8 km. A similar very small signal of less than 0.2×10^{-4} m^{-1} sr^{-1} was obtained at an altitude of about 6.5 km by the north probe instrument. A very small but significant fluctuation in the baseline signal, perhaps indicative of small amounts of scattering material, was noted for the day probe data from the main cloud deck base of about 49 km down to altitudes of about 30 km or lower. The hazes reported by Knollenberg and Hunten (*5*, *6*) in the 31- to 40-km region for the sounder probe location (of the order of one particle per cubic centimeter of radius 0.5 μm) do not have sufficient backscattering cross sections to be detected by our nephelometer.

The observations on particle indices and stratification at the sounder probe location are in essential agreement with those of Marov *et al.* (*4*), who have inferred cloud particle characteristics from multiple-angle light-scattering experiments conducted during the Venera 9 and 10 missions. The nearly simultaneous measurements at four widely separated locations of the Pioneer Venus mission, including high and low latitudes and day and night locations, have indicated the planetary nature of the stratification as well as the local variability in the details of this stratification. The altitudes at which the various strata occur differ by a few kilometers from one probe site to another, and the backscattering profiles of the lowest cloud regions (region B), which interact most strongly with light, are different at each location.

Marov *et al.* (*4*) have also reported obtaining strong signals in their backscattering nephelometer channels during the descent of the Venera probes into the lower portion of the atmosphere of Venus below the main cloud base. At the time of this publication the difference between our results and those of Marov *et al.* are unexplained.

The nephelometer experiments also embodied two channels for measuring ambient radiation, a "visible" channel centered at about 530 nm with a passband of about 70 nm full width at half maximum and a UV channel centered at 365 nm with a passband of 40 nm full width at half maximum. The UV channel

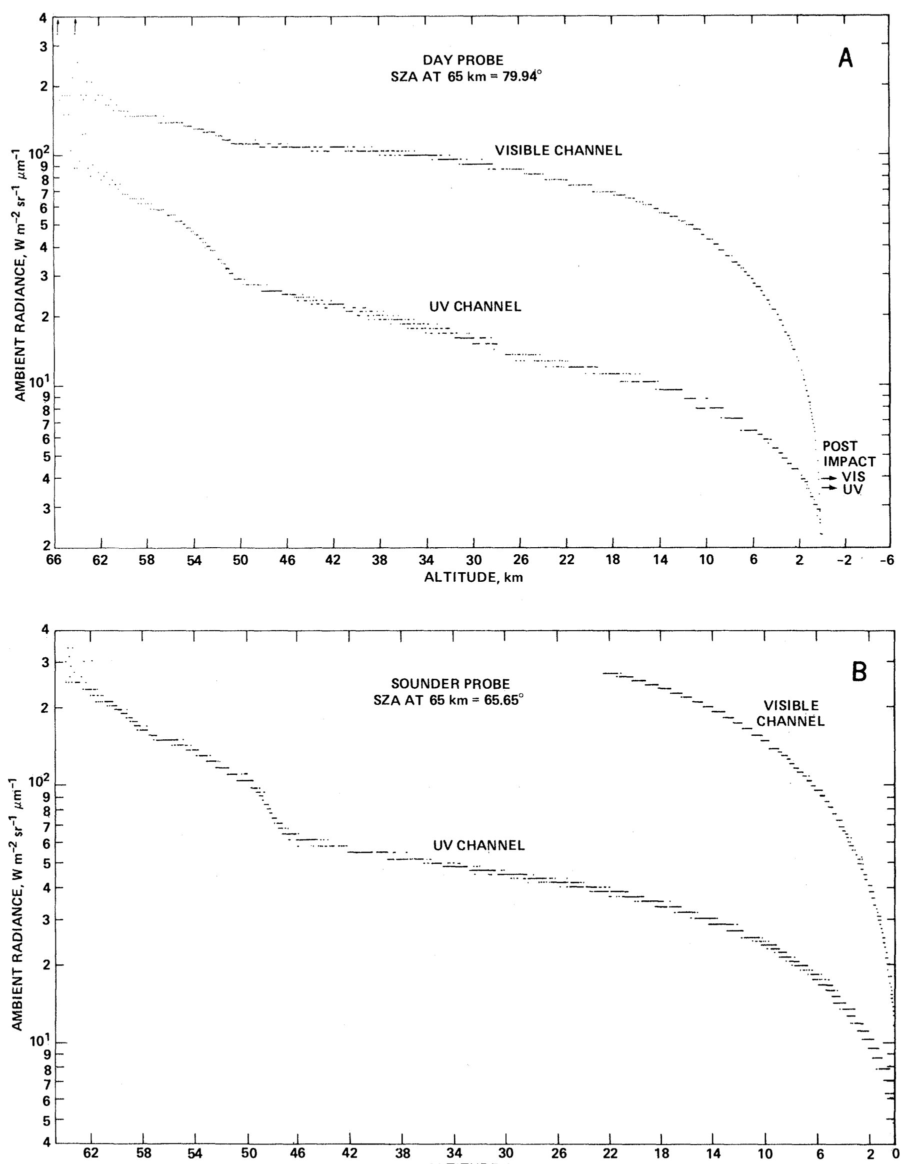

Fig. 2. Plots of ambient radiance versus altitude for the visible and UV channels. Altitudes have been referenced to the elevation of the impact location of the sounder probes. Absolute values of radiance are under continuing investigation and should be used with caution. (A) For the day probe, the observation angle is 98.5° with respect to the upstream-facing probe axis of symmetry, and the fields of view are approximately 11.5° to half-responsivity points. Ultraviolet and visible channels are separated in azimuth by 9°. (B) The observation angle for the sounder probe is 94.5° with respect to the upstream-facing probe axis, and the fields of view are approximately 11.5° to half-responsivity points. Visible and UV channels are separated in azimuth by 9°. No visible-channel data above 23 km are available for this probe.

was also found to have a response at 745 nm with a passband of 30 nm full width at half maximum and a response of about 28 percent of that of the 365-nm channel when exposed to a source whose power output was constant with wavelength.

The radiation data obtained as a function of altitude for the day probe and sounder probe are shown in Fig. 2 for the UV and the visible channels. Work is in progress on the absolute scales of the radiances, and, at present, such values should be used with caution. The relative behavior of these radiances, however, is as shown. As a first approximation, the altitude dependence of the UV intensity in the 365-nm passband has been determined by assuming that the altitude behavior of the portion of the signal in the UV channel attributed to 745-nm light is identical to that of the 530-nm radiation. Making this correction to the signal in the UV channel for the day probe, we obtain the data of Fig. 3, which indicate that very little UV light remains at altitudes below 25 to 30 km. For the remainder of the probe descent, it is thus possible to consider that the signal in the UV channel is due to 745-nm radiation, and its behavior may be compared with the visible channel behavior.

From the ambient radiation data, the following conclusions can be inferred.

1) The strong variations at the cloud tops are attributed to probe rotation and cloud patchiness.

2) In the cloud region, the stronger interaction of near-UV (as compared with visible) light is apparent. The variation of the slopes and of the second derivatives of the data agree with the general structure for the cloud regions determined from the backscatter data. The strongest rate of extinction occurs in the region extending from the highest altitudes measured down to 58 km. High extinction rates are also observed in the region from 56 to 50 km in the main cloud bank (regions C and B). Because of the apparent absence at the day probe location of the upper part of region B—so prominent at the sounder probe location—more UV light appears to penetrate to below the cloud at the day probe location than at the sounder probe location, as inferred from the fractional decrease in the UV signals passing through the cloud regions.

3) Below the clouds, extinction of the 365-nm channel radiation occurs down to about 26 km; near-UV light is present in all this part of the atmosphere. The near-UV light which had not been absorbed by heavy region B clouds is now propagated through and attenuated by the atmosphere down to about 26 km. Multiple scattering calculations are in progress (*7*) to help elucidate these data.

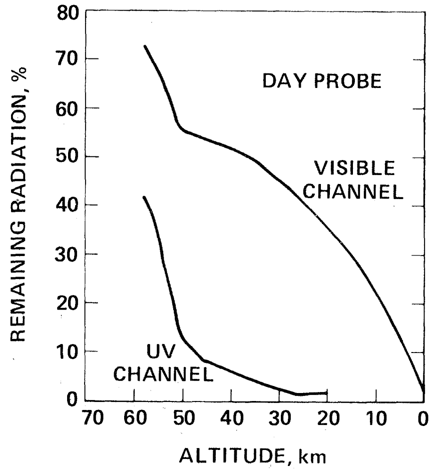

Fig. 3. Percentages of readings remaining for the UV (365-nm) channel of the day probe after correction for the 745-nm contribution. Also plotted are percentages of the readings remaining at each altitude for the 530-nm channel of the same probe; the assumed behavior for the 745-nm contribution (valid down to 25 to 30 km) to the UV channel follows this curve.

4) If the radiation remaining at 26 km as detected by the UV channel is primarily at a wavelength of 745 nm, the faster rate of change with altitude of the 530-nm radiance compared to the 745-nm radiance is evident. Golovin *et al.* (*8*) have observed that radiation in spectral regions below 600 nm is strongly absorbed starting below 20 km, an extinction perhaps attributable to molecular vapors such as sulfur or bromine. Calculations are in progress for our data to separate the Rayleigh scattering contributions to our signals in order to confirm this absorption.

JACQUES BLAMONT

Service d'Aeronomie du Centre National de la Recherche Scientifique, 91 Verrieres, France

BORIS RAGENT

NASA Ames Research Center, Moffett Field, California 94035

References and Notes

1. B. Ragent and J. Blamont, *Science* **203**, 790 (1979).
2. L. Colin and C. F. Hall, *Space Sci. Rev.* **20**, 283 (1977); L. Colin and D. Hunten, *ibid.*, p. 471.
3. Altitude profiles used in this report were obtained from A. Seiff [see A. Seiff, D. B. Kirk, R. E. Young, S. C. Sommer, R. C. Blanchard, J. T. Findlay, G. M. Kelly, *Science* **205**, 46 (1979)].
4. M. Ya. Marov, V. E. Lystsev, V. N. Lebedev, *USSR Academy of Sciences Reprint 144* (1978); M. Ya. Marov *et al.*, *Astron. J. Acad. Sci. USSR* **5** (No. 1) (1979).
5. R. Knollenberg and D. Hunten, *Science* **203**, 792 (1979).
6. ———, *ibid.* **205**, 70 (1979).
7. J. B. Pollack *et al.*, *ibid.*, p. 76.
8. Yu. M. Golovin, V. I. Moroz, B. E. Moshkin, N. A. Parfentiev, N. F. Sanko, A. P. Ekonomov, *Astron. J. Acad. Sci. USSR* **5** (No. 1) (1979).

9. We thank J. Bader, C. W. Clark, and W. Gunter of Ames Research Center; C. Cot of Service d'Aeronomie; and J. Gibson, J. Hunter, and T. McCarthy of Informatics, Inc., for support in data processing and instrument calibration.

15 May 1979

Clouds of Venus: A Preliminary Assessment of Microstructure

Abstract. *The multimodal microstructure of the Venus cloud system has been examined. In addition to confirmed H_2SO_4 droplets and suspected elemental sulfur, a highly concentrated aerosol population has been observed extending above, within, and below the cloud system. These aerosols appear to cycle through the cloud droplets, but can never be removed by the weak precipitation mechanisms present. All cloud particles are likely laced with aerosol contaminants. Sedimentation and decomposition of H_2SO_4 in the droplets of the lower cloud region contribute more than 7 watts per square meter of heat flux equaling one-fourth of the solar net flux at 50 kilometers.*

The particle-size distribution measurements by the Pioneer Venus large cloud particle size spectrometer (LCPS) revealed that the Venus cloud populations were inherently multimodal (*1*). Three modes are observed in the raw data centered approximately at 1, 3, and 8 μm diameter in the number density spectra. Table 1 summarizes the populations observed in each of three cloud and one haze regions. We have indicated that the observed multimodal size distributions were of fundamental importance with each mode suggesting different chemical composition or at least a different origin (*2*). Continuing reduction of Pioneer Venus results requires only slight adjustment of our ideas on the identities of the three groups of particles. It has become apparent, with final data on the descent profile of the probe, that temperatures are higher than was originally supposed, which raises questions of just how dilute the H_2SO_4 can be in the lower cloud region. Optical absorption data from the large probe solar net flux radiometer (LSFR) have provided additional constraints on the probability that mode 3 in the middle cloud region is elemental sulfur.

We have sought to separate and examine these modes in detail, treating them as distinct sizes as well as combined populations. The analysis involves removing